

JAAS

Accepted Manuscript



This is an *Accepted Manuscript*, which has been through the Royal Society of Chemistry peer review process and has been accepted for publication.

Accepted Manuscripts are published online shortly after acceptance, before technical editing, formatting and proof reading. Using this free service, authors can make their results available to the community, in citable form, before we publish the edited article. We will replace this *Accepted Manuscript* with the edited and formatted *Advance Article* as soon as it is available.

You can find more information about *Accepted Manuscripts* in the [Information for Authors](#).

Please note that technical editing may introduce minor changes to the text and/or graphics, which may alter content. The journal's standard [Terms & Conditions](#) and the [Ethical guidelines](#) still apply. In no event shall the Royal Society of Chemistry be held responsible for any errors or omissions in this *Accepted Manuscript* or any consequences arising from the use of any information it contains.

To be submitted to the *Journal of Analytical Atomic Spectrometry*

A special volume for the 2013 Goldschmidt conference (Florence, Italy)

Themed issue on “Geological application of laser ablation”

Feb. 28th 2014

***In situ* U-Pb dating of bastnaesite by LA-ICP-MS**

Yue-Heng, Yang^{a*}, Fu-Yuan, Wu^a, Yang, Li^{a,b}, Jin-Hui, Yang^a, Lie-Wen, Xie^a, Yan, Liu^c, Yan-Bin, Zhang^a, Chao, Huang^a

^a State Key Laboratory of Lithospheric Evolution, Institute of Geology and Geophysics, Chinese Academy of Sciences, P. B. 9825, Beijing, 100029, P. R. China

^b School of Earth Sciences, Graduate University of Chinese Academy of Sciences, Beijing, 100039, P. R. China

^c Institute of Geology, Chinese Academy of Geological Sciences, Beijing, 100037, P. R. China

* Corresponding author. Tel: +86-010-82998599 Fax: +86-010-62010846

E-mail: yangyueheng@mail.iggcas.ac.cn

1
2
3
4 20 **Abstract** Bastnaesite, a common accessory mineral in REE ore deposits, is ideal for U-Pb isotopic
5
6 21 dating because of its relatively high U and Th contents. We report an analytical procedure for U-Pb
7
8 22 dating of this mineral using an 193 nm ArF excimer laser ablation system coupled to an Agilent
9
10 23 7500a (LA-ICP-MS). Laser-induced elemental fractionation and instrumental mass discrimination
11
12 24 were externally corrected using an in-house bastnaesite standard (K-9). The fluence, spot size and
13
14 25 repetition rate of laser was evaluated to assess their effects on age determination in detail. The matrix
15
16 26 effect on zircon and bastnaesite was also investigated and compared in full during laser sampling.
17
18 27 The results indicate that a matrix-matched standard reference material is essential. In order to
19
20 28 validate and demonstrate the effectiveness and robustness of our developed protocol, we dated
21
22 29 several bastnaesite samples from the Himalayan Mianning-Dechang REE belt, South-West China.
23
24 30 The U-Pb ages of ~ 31 to 34 Ma obtained on bastnaesites from the Maoniuping, Diaoloushan,
25
26 31 Zhengjialiangzi and Lizhuang, are in good agreement within error, but differ from the wide range of
27
28 32 age (10 – 40 Ma) obtained using K-Ar and Ar-Ar method on biotite and muscovite and U-Pb in
29
30 33 zircon. These dating applications demonstrate the reliability and feasibility of our established method.
31
32 34 In summary, the LA-ICP-MS dating of bastnaesite can be a complementary dating method to the
33
34 35 more established TIMS and SIMS technique with its advantages of rapidity, moderate spatial
35
36 36 resolution and relatively low cost.
37
38
39
40
41
42
43
44
45
46
47
48

49 **Keywords** Bastnaesite; REE deposits; U-Th-Pb isotopic dating; LA-ICP-MS
50
51
52
53

54 1. Introduction

55
56 41 The ability to accurately determine the time of mineralization is crucial for understanding the
57
58
59
60

1
2
3
4 42 genesis of endogenous ore deposits and forming processes.¹ According to the present knowledge,
5
6 43 numerous radiometric dating methods have been applied to date mineralization, including K (Ar)-Ar,
7
8
9 44 Rb-Sr, Sm-Nd, Lu-Hf, Re-Os and U-Pb techniques. Among these techniques, U-Pb method has been
10
11 45 considered as the most powerful tool to get precise and accurate age of mineralization. However, for
12
13 46 most ore deposits, U-Pb method is not applicable due to the lack of suitable minerals. This problem
14
15
16 47 is also encountered in dating rare earth element (REE) deposits which is generally related to the
17
18
19 48 occurrences of alkaline and carbonatite rocks.¹⁻³

20
21 49 Bastnaesite (Bastnäsite, $(\text{Ce})\text{CO}_3\text{F}$), a carbonate-fluoride mineral, is a common accessory
22
23 50 mineral in REE ore deposits and it was firstly described by the Swedish chemist Wilhelm Hisinger in
24
25
26 51 1838 and named after the Bastnäs mine near Riddarhyttan, Västmanland, Sweden. This mineral can
27
28
29 52 occur as very high quality specimens (Zagi Mountains, Pakistan), but mostly it occurs in alkali
30
31 53 granite, syenite and associate pegmatite, and carbonatite. The mineral has a variable composition
32
33
34 54 among La, Ce, Nd, Y and Ba, and forms a group mineral of bastnaesite, parasite, cordylite,
35
36
37 55 Huangheite, cebaite and Zhonghuacerite. Whatever, bastnaesite is one of the most important REE
38
39 56 carriers as monazite (Mountain Pass in USA, and Bayan Obo in China). In contrast to monazite,
40
41 57 however, bastnaesite is less investigated for its U-(Th)-Pb and other isotopic systems, despite its
42
43
44 58 fairly wide occurrence or distribution in carbonatites, alkaline rocks, and associated REE deposits.²⁻⁵

45
46 59 To the best of our knowledge, bastnaesite has been dated using La-Ba method by traditional
47
48
49 60 isotopic dilution thermal ionization mass spectrometer (ID-TIMS).⁶ Using this method, an isochron
50
51 61 age of 586.8 ± 3.7 Ma was obtained for the bastnaesite from Gakara deposit in Burundi. The
52
53
54 62 pioneering works on the Bayan Obo deposit by Wang et al.² indicated that bastnaesite there contains
55
56
57 63 much less amount of U (mostly less than 0.5 ppm), which makes unavailable to get its U-Pb age,
58
59
60

1
2
3
4 64 although a Th-Pb age of 555 to 475 was obtained. Considering that the associated monazite contain
5
6 65 extremely low amount of U as well, it is unknown that whether bastnaesite in other area contain the
7
8
9 66 similar level of U concentration. Recently, however, Salnikova et al.⁴ conducted a U-Pb isotopic
10
11 67 analysis for the bastnaesite from the Karasug carbonatite in central Mongolia, and obtained a
12
13 68 concordant age of 118 ± 1 Ma. Therefore, it was demonstrated that bastnaesite could be an important
14
15 69 mineral to constrain the age of REE mineralization. It is also interesting to note that the obtained
16
17 70 $^{206}\text{Pb}/^{204}\text{Pb}$ ratios for the two analyses are 488 (U of 222 ppm) and 1440 (U of 653 ppm), respectively,
18
19 71 which corresponds to 3.8% and 1.3% of f_{206} ratios. Considering that the studied samples were formed
20
21 72 in the Mesozoic, most bastnaesite, especially those formed in Precambrian, might have low to
22
23 73 negligible common lead, as usually dated minerals of zircon, baddeleyite, monazite and xenotime.
24
25 74 However, most REE deposits have a complicated history due to intensive fluid activities. For
26
27 75 example, the Bayan Obo, the most important REE deposit in the world, is still in debate for its
28
29 76 formation age due to later alteration.^{2,3} In this case, *in situ* U-Pb analytical technique is desired to
30
31 77 decipher the complex history of the REE mineralization.
32
33
34
35
36
37
38

39 78 In addition, the crystal structure of bastnaesite can accommodate high concentrations of light
40
41 79 rare earth elements (LREE), with Nd content of ~10 wt %, which makes it an ideal candidate for *in*
42
43 80 *situ* Nd isotopic analyses.⁵ This kind of data would definitively provide important information on the
44
45 81 origin and genesis of the ore deposits¹. Therefore, in this study, we developed an *in situ* protocol of
46
47 82 U-Pb dating bastnaesite by LA-ICP-MS and explored its application as a dating method. The fluence,
48
49 83 spot size and repetition rate of laser was evaluated to check the age of bastnaesite in detail. The
50
51 84 matrix effect on zircon and bastnaeiste was also investigated. The reliability and validity of the
52
53 85 proposed methodology have been tested by using samples of bastnaesite collected in the Himalayan
54
55
56
57
58
59
60

1
2
3
4 86 Mianning-Dechang REE belt, South-West China. These samples were previously dated by
5
6 87 conventional Rb-Sr, Ar-Ar and U-Pb dating methods. Our results indicate that bastnaesite can
7
8
9 88 contain a significant amount of common Pb, therefore indicate a common Pb correction is necessary
10
11 89 in order to give a correct U-Pb age, which differs from the previous observation.¹
12
13
14 90

16 91 **2. Experimental**

18
19 92 All bastnaesite samples investigated in this work were analyzed for major, trace element
20
21 93 concentration and U-Th-Pb ages by *in situ* LA-ICP-MS techniques. All analyses were conducted at
22
23 94 State Key Laboratory of Lithospheric Evolution at the Institute of Geology and Geophysics, Chinese
24
25 95 Academy of Sciences, Beijing.
26
27
28
29 96

31 97 **2.1. Sample preparation**

33
34 98 All bastnaesite grains were mounted in epoxy in 2.5 cm diameter circular grain mounts and
35
36 99 polished until the bastnaesite grains were just revealed. Transmitted, reflected and back-scattered
37
38
39 100 electron microscopic images were used to examine the internal structure, such as inclusions, crack
40
41 101 and growth zones which provide a base map for selection of ablation spots. The grain mount was
42
43
44 102 cleaned and left in 2% HNO₃ for several min prior to laser ablation analysis.⁷
45
46
47 103

49 104 **2.2. Bastnaesite reference material**

51 105 Well-characterized matrix-matched reference material is crucial for *in situ* analytical technique.
52
53
54 106 Unlike other widely distributed and well characterized mineral standards such as zircon (*e.g.*, 91500,
55
56 107 etc.), monazite (*e.g.*, 44069, etc), apatite (*e.g.*, Durango, etc) and titanite (*e.g.*, BLR-1 etc), so far,
57
58
59
60

1
2
3
4 108 there no reported reference material of bastnaesite for in situ laser ablation. The primary bastnaesite
5
6 109 *in-house* reference standard analyzed in this study was K-9, which has yielded a TIMS concordian
7
8
9 110 age of 118 ± 1 Ma (MSWD = 0.05, probability = 0.82). This standard was collected from the
10
11 111 supergene altered hematite-bearing siderite carbonatite with baritocelastine. Moreover, its ID-TIMS
12
13 112 U-Pb age is in agreement with the Sm-Nd ages obtained on bastnaesite and fluorite from the
14
15 113 carbonatite, and is also consistent with the age of 118 ± 9 Ma obtained by the Rb-Sr method on mica
16
17 114 from carbonatites. A detailed description on samples location can be found in Salnikova et al.⁴
18
19
20
21
22
23

24 116 2.3. Instrumentation

25
26 117 **Table 1**

27
28
29 118 Experiments were carried out using an Agilent 7500a ICP-MS (Agilent Technologies, Japan) in
30
31 119 combination with an excimer 193 nm laser ablation system (Geolas 2005, Lambda Physik, Gottingen,
32
33 120 Germany). The laser spot size was adjusted to 5, 10, 16, 24, 32, 44, 60, 90, 120 and 160 μm and the
34
35 121 frequency can be adjusted from 1 to 20 Hz.⁸
36
37
38
39
40

41 123 2.4. Mass spectrometry

42
43
44 124 The analytical procedure for bastnaesite U-Th-Pb dating and trace elements compositions
45
46 125 (including REE) is similar to the zircon, monazite and apatite dating by LA-ICP-MS. A summary of
47
48 126 the LA-ICP-MS specifications and typical operating conditions used in this study are presented in
49
50 127 Table 1. Helium was used as the carrier gas through the ablation cell and was merged with argon
51
52 128 (make-up gas) downstream the ablation cell.⁹ Prior to analysis, the Pulse/Analogy (P/A) factor of the
53
54
55 129 detector was calibrated using standard tuning solution. The carrier and make-up gas flows were
56
57
58
59
60

1
2
3
4 130 optimized to obtain maximum signal intensity for $^{238}\text{U}^+$, while keeping the ThO^+/Th^+ ratio below
5
6 131 0.5%. All LA-ICP-MS measurements were carried out using time resolved analysis in fast, peak
7
8
9 132 jumping mode. Each spot analysis consists of an approximate 20 s background acquisition and a 65 s
10
11 133 sample data acquisition. The dwell time for each isotope was set at 6 ms for Rb, Sr, Ba, Nb, Ta, Zr,
12
13 134 Hf and REE, 10 ms for ^{232}Th , ^{238}U , 15 ms for ^{204}Pb , ^{206}Pb , ^{208}Pb , and 30 ms for ^{207}Pb . A
14
15 135 matrix-matched external bastnaesite standard (K-9) was used to correct for U-Th-Pb fractionation
16
17 136 and instrumental mass discrimination. Two K-9 analyses were measured after every five unknown
18
19 137 bastnaesite spot. In this work, the cratering model rather than rastering ablated model was adopted
20
21 138 and the total ablated time took about 60 second for a single standard or sample measurement.
22
23
24
25
26
27
28

29 140 **2.5. Data reduction**

30
31 141 Signals of ^{204}Pb , ^{206}Pb , ^{207}Pb , ^{208}Pb , ^{232}Th and ^{238}U were acquired for U-Pb dating, whereas the
32
33 142 ^{235}U signal was calculated from ^{238}U on the basis of the ratio $^{238}\text{U}/^{235}\text{U} = 137.88$. All the measured
34
35 143 $^{207}\text{Pb}/^{206}\text{Pb}$, $^{207}\text{Pb}/^{235}\text{U}$ and $^{206}\text{Pb}/^{238}\text{U}$ isotopic ratios of the K-9 standard during the process of sample
36
37 144 analyses were regressed and corrected using the reference values. The concordia age of 118 Ma was
38
39 145 used as the reference value.⁴ Standard deviations of the calibrated isotope ratios include those from
40
41 146 sample, external standard, and deviations from the reference values of external standard. The
42
43 147 uncertainty was set at 2 %. The U-Pb concordia ages and weighted mean ages were calculated using
44
45 148 the ISOPLOT/EX 3.23 software package.¹⁰ Trace concentrations were calibrated against the NIST
46
47 149 SRM 610 as external reference material using ^{140}Ce as an internal standard using the Glitter
48
49 150 software.¹¹ Ce was used as an internal standard for calibration purpose.
50
51
52
53
54
55

56 151 Accurate correction for laser-induced elemental fractionation and instrumental drift is an
57
58
59
60

1
2
3
4 152 important consideration in U-Pb dating of accessory minerals in LA-ICP-MS measurement. In this
5
6 153 study, we used the well characterized matrix-matched in-house K-9 standard protocol to correct for
7
8
9 154 U-Pb elemental fractionation and variations in sensitivity during an analytical session. The procedure
10
11 155 is similar to the one used for zircon dating by LA-ICP-MS with GJ-1 or 91500 standard.^{11,12} Another
12
13 156 significant difficulty of U-Pb dating of bastnaesite is the present high common Pb content, which is
14
15
16 157 incorporated from the parental magma in the early phase of mineral crystallization.¹³ As recently
17
18 158 noted by Chew et al.¹³, common Pb correction is typically undertaken using either concordia or
19
20
21 159 isochron plots on a suite of co-genetic grains or alternatively on individual analyses using an
22
23 160 appropriate choice of initial Pb isotopic composition. In this study, the ²⁰⁷Pb correction method was
24
25
26 161 applied for common Pb correction using the two-stage model of Stacey and Kramers¹⁵ (refer also to
27
28 162 Williams¹⁶) and the ²⁰⁶Pb/²³⁸U weighted ages were calculated using Isoplot 3.23. Moreover, the
29
30
31 163 intercepts of regression line through the raw data on a Tera-Wasserburg plot provide an estimate of
32
33 164 the ²⁰⁷Pb/²⁰⁶Pb for the common Pb component (upper intercept) and the inferred crystallization age
34
35
36 165 (lower intercept).^{17,18}

37
38
39
40
41
42
43
44
45
46
47
48
49
50
51
52
53
54
55
56
57
58
59
60

167 **3. Results and discussion**

168 **3.1. Matrix effect**

169 **Figure 1**

170 The lack of well-characterized matrix-matched reference materials to correct for elemental
171 fractionation is significant obstacle for *in situ* U-Pb dating of accessory minerals by LA-ICP-MS or
172 SIMS techniques. Therefore, we first evaluated the matrix effect on *in situ* U-Pb age analysis of
173 bastnaesite (K-9) and zircon (GJ-1) reference materials using zircon standard 91500 as external

1
2
3
4 174 calibrating standard during the same analytical session. When the 91500 zircon was used as external
5
6 175 calibration standard, the obtained weighted $^{206}\text{Pb}/^{238}\text{U}$ age for the K-9 standard is 107.86 ± 0.89 Ma
7
8
9 176 (MSWD = 0.83, n = 18, Fig. 1a), which is 10 % younger than the published reference value of $118 \pm$
10
11 177 1 Ma.⁴ However, the weighted $^{206}\text{Pb}/^{238}\text{U}$ age of 611.0 ± 5.7 Ma (MSWD = 0.76, n = 18, Fig. 1b) for
12
13
14 178 GJ-1 agrees well with the published recommended value using ID-TIMS (608.53 ± 0.37 Ma).²³
15
16 179 Similarly, if bastnaesite K-9 was used as external calibration standard, the weighted $^{206}\text{Pb}/^{238}\text{U}$ age of
17
18
19 180 K-9 as a unknown sample is 118.0 ± 1.0 Ma (MSWD = 0.66, n = 18), in good agreement with the
20
21 181 classic ID-TIMS data.⁴ However, the weighted $^{206}\text{Pb}/^{238}\text{U}$ age (666.9 ± 6.5 Ma, MSWD = 0.94, n =
22
23
24 182 18) of GJ-1 is 10% older than the reference value.²³ These results means that there are significant
25
26 183 matrix effects between bastnaesite and zircon during laser ablation, indicating that a suitable
27
28
29 184 matrix-matched standard is essential and crucial for *in situ* U-Pb dating of bastnaesite using
30
31 185 LA-ICP-MS. Although the exact reason for significant matrix effect is still unknown, the similar
32
33
34 186 situation had been previously observed and reported for titanite, allanite, xenotime, monazite and
35
36 187 zircon during *in situ* U-Pb dating by LA-ICP-MS technique.¹⁹⁻²²
37
38
39 188

40 41 189 **3.2. Laser spot size, repetition rate and fluence**

42 43 44 190 **Figure 2**

45
46 191 Ablation experiments on the bastnaesite (K-9) grain were carried out using a spot ablation
47
48
49 192 routine at repetition rates of 4, 6, 8 and 10 Hz and on sample fluences of 4, 6, 8 and 10 J/cm². Spot
50
51 193 sizes of 16, 32, 44 and 60 μm were used to obtain enough intensity for the less abundant isotopes,
52
53
54 194 and to avoid potential zonation. As shown in Figure 2 a, b, c & d and Table 2, at a constant repetition
55
56 195 rate of 8 Hz and 44 μm crater size, with increasing fluences of 4, 6, 8 and 10 J/cm², the obtained
57
58
59
60

1
2
3
4 196 weighted $^{206}\text{Pb}/^{238}\text{U}$ ages of K-9 for every ten analyses are 125.5 ± 2.0 Ma (MSWD = 1.07, 4 J/cm²),
5
6 197 116.9 ± 1.6 Ma (MSWD = 0.73, 6 J/cm²), 117.3 ± 1.5 Ma (MSWD = 0.50, 8 J/cm²) and 117.4 ± 1.5
7
8 198 Ma (MSWD = 0.33, 10 J/cm²), respectively. Similarly, as shown in Figure 2 e, f & g, at a constant
9
10 199 repetition rate of 8 Hz and fluence of 8 J/cm², with increasing crater size 16, 32 and 60 μm , the
11
12 200 above ages are 120.3 ± 4.8 Ma (MSWD = 3.6, 16 μm), 119.4 ± 1.4 Ma (MSWD = 0.34, 32 μm) and
13
14 201 119.5 ± 1.2 Ma (MSWD = 1.18, 60 μm), respectively. Additionally, as shown in Figure 2 h, i & j, at a
15
16 202 constant fluence of 8 J/cm² and 44 μm crater size, with increasing repetition rate from 4, 6 and 10 Hz,
17
18 203 our obtained weighted $^{206}\text{Pb}/^{238}\text{U}$ ages of ten analyses for each are 116.9 ± 2.1 Ma (MSWD = 1.9,
19
20 204 4Hz), 117.1 ± 1.2 Ma (MSWD = 0.50, 6Hz) and 118.0 ± 1.2 Ma (MSWD = 0.92, 10Hz), respectively.
21
22 205 The above experiments indicate that there is no significant age variations with variable spot size,
23
24 206 repetition rate and fluence intensity. As shown in Figure 2 and Table 2, the spot size have more
25
26 207 significant effect on the age error than repetition rate and fluence because of its less ablated material
27
28 208 and less intensity signal (e.g., 16 μm). Therefore, a spot size of 44 μm was applied with a repetition
29
30 209 rate of 8 Hz, corresponding to an energy density of ~ 10 J/cm², these condition were applied to the
31
32 210 following samples analyses.
33
34
35
36
37
38
39
40
41
42

212 4. Application

213 Figure 3 & 4

214 In order to demonstrate the effectiveness and robustness of our developed protocol, we dated
215 numerous bastnaesite samples and compared with the results with available published data. The
216 bastnaesite grains were prepared following the procedure described in sample preparation. The
217 chemical compositions of these samples for REE contents were listed in Appendix and the REE

1
2
3
4 218 patterns are shown in Figure 3.

5
6 219 As well-known, the Himalayan Mianning-Dechang (MD) REE belt, western Sichuan, SW
7
8
9 220 China, is approximately 270 km long and 15 km wide, and contains total reserves of more than 3 Mt
10
11 221 of LREE, including one giant (Maoniuping), one large (Dalucao) and a number of small-medium
12
13 222 REE deposits (Moluozhai and Lizhuang).²⁴⁻²⁷ REE mineralization is associated with Himalayan
14
15 223 carbonatite-alkaline complexes, which consist of carbonatitic sills or dykes and associated alkaline
16
17 224 syenite stocks. A few available dating data define a Himalayan metallogenic epoch (10 – 40 Ma) by
18
19
20
21 225 K-Ar or Ar-Ar method on biotite and muscovite or U-Pb dating of zircon by SHRIMP.²⁵⁻²⁷
22

23
24 226 The Maoniuping (MNP) is a world-class REE deposit, following only the Bayan Obo
25
26 227 REE-Nb-Fe (China) and Mountain Pass (USA) REE deposits in terms of size. Previously, K-Ar
27
28 228 dating of hydrothermal minerals (biotite and magnesio-arfvedonite) yielded a age ranging from 27.8
29
30
31 229 ± 0.5 Ma to 40.3 ± 0.7 Ma,²⁸ indicating relatively wide REE mineralization age for this deposit. The
32
33 230 analysed sample of MNP4256 contains ~ 11 ppm of U and ~ 2467 ppm of Th, with Th/U ratios of \sim
34
35 231 243. Twelve analyses yield a lower intercept age of 31.1 ± 3.9 Ma, which is identical to the ²⁰⁷Pb
36
37 232 corrected age of 30.7 ± 3.0 Ma (Fig. 4a). Therefore, we consider that this deposit was formed at ~ 31
38
39
40
41 233 Ma.
42

43
44 234 Muluozhai is composed by two small deposits of Diaoloushan (DLS) and Zhengjialiangzi
45
46 235 (ZJLZ). The obtained K-Ar ages from potassium feldspar and phlogpite are 31.2 and 35.5 Ma,
47
48 236 respectively. The analysed sample of DLS contains ~ 16 (DLS108), 12 (DLS110) ppm of U and \sim
49
50 237 2220 (DLS108), ~ 1603 (DLS110) ppm of Th, with Th/U ratios of ~ 144 (DLS108), ~ 136 (DLS110),
51
52 238 respectively. The obtained intercept ages are 32.2 ± 2.6 (DLS108) and 34.9 ± 3.1 Ma (DLS110), with
53
54
55 239 ²⁰⁷Pb corrected ages of 31.8 ± 2.1 (DLS108) and 33.0 ± 2.6 Ma (DLS110) (Figure 4b & c). For the
56
57
58
59
60

1
2
3
4 240 Zhengjialiangzi deposit, the analysed sample of ZJLZ103 contains ~ 7.8 ppm of U and ~ 1826 ppm
5
6 241 of Th, with Th/U ratios of ~ 272. Nineteen analyses for the sample yield intercept and ^{207}Pb corrected
7
8
9 242 ages of 33.3 ± 3.3 and 33.3 ± 2.6 Ma, identical to those obtained from the Maoniuping deposit.

10
11 243 Another deposit in the area is Lizhuang (LZ), which gives a K-Ar age ranging between 27.1 and
12
13 244 30.6 Ma. The analysed sample of LZ122 contains ~ 27 ppm of U and ~ 4555 ppm of Th, with Th/U
14
15 245 ratios of ~ 167. During this study, sample LZ122 was collected for its U-Pb analysis, the obtained
16
17 246 intercept and ^{207}Pb corrected ages are 32.9 ± 3.7 and 33.0 ± 2.1 Ma, respectively (Figure 4e),
18
19 247 consistent with those from the Maoniuping and Muluozhai deposits.

20
21 248 Dalucao (DLC) is the second largest deposit in the MD REE belt. The obtained K-Ar ages from
22
23 249 biotite and muscovite range from 9.8 to 14.5 Ma,²⁹ which is slightly younger than the Rb-Sr isochron
24
25 250 age of 15.3 ± 0.5 Ma for REE ores. U-Pb dating of zircons from carbonatite and syenite yielded age
26
27 251 of 12.99 ± 0.94 and 14.53 ± 0.31 Ma, respectively.²⁶ Our analysed sample of DLC43 contains ~ 3.0
28
29 252 ppm of U and ~ 475 ppm of Th, with Th/U ratios of ~ 158. Twelve analyses on this sample yield a
30
31 253 lower intercept age of 21.9 ± 5.9 Ma, with ^{207}Pb corrected age of 20.8 ± 4.9 Ma (Figure 4f), about 10
32
33 254 Ma younger than those from other deposits presented above. However, it is noted that the obtained
34
35 255 ages from this sample show large errors than other samples studied due to its lower U concentration.

36
37 256 The age data presented above indicated that all of the deposits in the area were synchronously
38
39 257 formed at ~31-34 Ma, consistence with the K-Ar or Ar-Ar ages for most deposits, except of Dalucao.
40
41 258 For the latter, our U-Pb age is significant older than the reported K-Ar, Rb-Sr and U-Pb ages.
42
43 259 Although this discrepancy needs more analyses to be verified, the consistence of ages among other
44
45 260 deposits suggests that our data are reliable. This practical dating example demonstrated the
46
47 261 applicability and promising prospect of our developed methodology for commonly
48
49
50
51
52
53
54
55
56
57
58
59
60

1
2
3
4 262 bastnaesite-bearing carbonatite, alkaline rocks and related REE deposits in the near future.¹
5
6 263 Moreover, it is noted from the data that our samples contain significant common lead although exact
7
8
9 264 amounts are not available from laser ablation analyses.
10
11 265

12 13 14 266 **5. Conclusions**

15
16 267 In this contribution, we demonstrated the possibility of bastnaesite as a dating mineral for U-Pb
17
18 268 geochronology using the LA-ICP-MS. The relatively easy sample preparation and operating system
19
20
21 269 combined with the short running time make it an ideal mineral for dating bastnaesite-bearing rocks.
22
23 270 Laser-induced elemental fractionation and instrumental mass discrimination were externally
24
25
26 271 corrected using the reference material K-9. The laser fluence, spot size and repetition rate was
27
28
29 272 evaluated to assess the quality of the obtained age in detail. The matrix effect on zircon and
30
31
32 273 bastnaesite was investigated and compared in detail during laser sampling. Our result indicates that
33
34 274 the matrix effects between bastnaesite and zircon maybe significant. In order to validate and
35
36 275 demonstrate the efficacy and strength of our developed protocol, we tested the *in situ* U-Pb dating
37
38
39 276 application on several bastnaesite samples collected in SW China, which show the reliability of our
40
41
42 277 established method. The minerals of the bastnaesite group have a fairly wide distribution and a
43
44 278 relatively high U and Th Pb contents making it an ideal mineral for U-Pb isotopic dating
45
46 279 LA-ICP-MS can be considered a promising geochronological tool suitable for U-Pb dating of
47
48
49 280 carbonatites, alkaline rocks, and related REE deposits.
50

51 281

52 53 54 282 **Acknowledgements**

55
56 283 This study was financially supported by the Natural Science Foundation of China (NSFC Grants
57
58
59
60

1
2
3
4 284 41273021, 41221002 and 41130313). We are greatly indebted to Dr. E. B. Sal'Nikova for kindly
5
6 285 providing the K-9 bastnaeite standard. We are particularly thankful to Dr. Yamirka
7
8 286 Rojas-Agramonte for correcting the English. We also thank Laura Petley for her patient while
9
10 287 handling our manuscript and also grateful for the critical and insightful comments from two
11
12 288 anonymous referees who improved the quality of the manuscript.
13
14

15 16 289 **References**

- 17
18 290 1. Robert, F., 1990. *Nature* **364**, 792–793.
- 19
20 291 2. Wang, J. W., Tatsumoto, M., Li, X. B., Premo, W. R., Chao, E. C. T., 1994. *Geochimica et*
21
22 292 *Cosmochimica Acta* **58**, 3155–3169.
- 23
24 293 3. Ling, M. X., Liu, Y. L., Williams, I. S., Teng, F. Z., Yang, X. Y., Ding, X., Wei, G. J., Xie, L.
25
26 294 H., Deng, W. F., Sun, W. D., 2013. *Scientific Report* **3**, 1776, DOI: 10.1038/srep01776.
- 27
28 295 4. Sal'Nikova, E. B., Yakovleva, S. Z., Nikiforov, A. V., Kotov, A. B., Yarmolyuk, V. V., Anisimova,
29
30 296 I. V., Sugorakova, A. M., Plotkina, Yu. V. 2010. *Doklady Earth Sciences* **430**, 134–136.
- 31
32 297 5. Yang, Y. H., Wu, F. Y., Fan, H. R., Xie, L. W., Zhang, Y. B. 2009a. *Geochimica et Cosmochimica*
33
34 298 *Acta* **73**, A1481.
- 35
36 299 6. Nakai, S., Masuda, A., Lehmann E. 1988. *American Mineralogist* **73**, 111–113.
- 37
38 300 7. Wu, F. Y., Yang, Y. H., Xie, L. W., Yang, J. H., Xu, P., 2006. *Chemical Geology* **234**, 105–206.
- 39
40 301 8. Xie, L. W., Zhang, Y. B., Zhang, H. H., Sun, J. F., Wu, F. Y., 2008. *Chinese Science Bulletin* **53**,
41
42 302 1565–1573.
- 43
44 303 9. Günther, D., Heinrich, C.A., 1999. *Journal of Analytical Atomic Spectrometry* **14**, 1363–1368.
- 45
46 304 10. Ludwig, K.R., 2003. A geochronological toolkit for microsoft excel. *Isoplot*, **3**, 1-70.
- 47
48 305 11. Griffin, W.L., Powell, W.J., Pearson, N.J., O'Reilly, S.Y., 2008. *Mineralogical Association*
49
50
51
52
53
54
55
56
57
58
59
60

- 1
2
3
4 306 *Canada Short Course* **40**, 308–311.
- 5
6 307 12. Košler, J., Fonneland, H., Sylvester, P., Tubrett, M., Pedersen, R.B., 2002. *Chemical Geology*
7
8 308 **182**, 605–618.
- 9
10
11 309 13. Chew, D. M., Petrus, J. A., Kamber, B. S. 2014. *Chemical Geology* **363**, 185–199.
- 12
13
14 310 14. Cox, R. A., Wilton, R. H. C. 2006. *Chemical Geology* **235**, 21–32.
- 15
16 311 15. Stacey, J.S., Kramers, J.D., 1975. *Earth and Planetary Science Letters* **26**, 207–221.
- 17
18
19 312 16. Williams, I.S., 1998. U–Th–Pb geochronology by ion microprobe. In: McKibben, M.A.,
20
21 313 Shanks III, W.C., Ridley, W.I. (Eds.), *Reviews in Economic Geology*, vol. 7, pp.1–35.
- 22
23
24 314 17. Batumike, J. M., Griffin, W. L., Belousova, E. A., Pearson, N. J., O' Reilly, S. Y., Shee, S. R.,
25
26 315 2008. *Earth and Planetary Science Letters* **267**, 609–619.
- 27
28
29 316 18. Yang, Y. H., Wu, F. Y., Wilde, S. A., Liu, X. M., Zhang, Y. B., Xie, L. W., Yang, J. H. 2009b.
30
31 317 *Chemical Geology* **264**, 24–42.
- 32
33
34 318 19. Sun, J. F., Yang, J. H., Wu, F. Y., Xie, L. W., Yang, Y. H., Liu, Z. C., Li, X. H. 2012. *Chinese*
35
36 319 *Science Bulletin* **57**, 2506–2516.
- 37
38
39 320 20. Liu, Z. C., Wu, F. Y., Guo, C. L., Zhao, Z. F., Yang, J. H., Sun, J. F. 2011. *Chinese Science*
40
41 321 *Bulletin* **56**, 2948–2956.
- 42
43
44 322 21. Korh, A. E. 2013. *Spectrochimica Acta Part B* **86**, 75–87.
- 45
46 323 22. Korh, A. E. 2014. *Chemical Geology* **371**, 46–59.
- 47
48
49 324 23. Jackson, S. E., Pearson, N. J., Griffin, W. L. Belousova, E. A. 2004. *Chemical Geology* **211**,
50
51 325 47–69.
- 52
53
54 326 24. Xu, C., Campbell, I. H., Kynicky, J., Allen, C. M., Chen, Y. J., Huang, Z. L., Qi, L. 2008. *Lithos*
55
56 327 **106**, 12–24.
- 57
58
59
60

- 1
2
3
4 328 25. Hou, Z. Q., Tian, S. H., Xie, Y. L., Yang, Z. S., Yuan, Z. X., Yin, S. P., Yi, L. S., Fei, H. C., Zou,
5
6 329 T. R., Bai, G., Li, X. Y. 2009. *Ore Geology Reviews* **36**, 65–89.
7
8
9 330 26. Tian, S. H., Hou, Z. Q., Yang, Z. S., Chen, W., Yang, Z. M., Yuan, Z. X., Xie, Y. L., Fei, H. C.,
10
11 331 Yin, S. P., Liu, Y. C., Li, Z., Li, X. Y. 2008a. *Mineral Deposits* **27**, 177–187 (*in Chinese with*
12
13 332 *English abstract*).
14
15
16 333 27. Tian, S. H., Hou, Z. Q., Yang, Z. S., Yang, Z. M., Yuan, Z. X., Wang, Y. B., Xie, Y. L., Liu, Y. C.,
17
18 334 Li, Z. 2008b. *Acta Petrologica Sinica* **24**, 544–554 (*in Chinese with English abstract*).
19
20
21 335 28. Yuan, Z. X., Shi, Z. M., Bai, G., Wu, C. Y., Chi, R. A., Li, X. Y. 1995. *Seismological Press,*
22
23 336 *Beijing*. 150 pp., (*in Chinese*).
24
25
26 337 29. Yang, G. M., Chang, C., Zuo, D. H., Liu, X. L. 1998. *Open file of China University of*
27
28 338 *Geosciences, Wuhan*, pp. 1–89 (*in Chinese*).
29
30
31 339

340 **Figure Captions**

341
342 **Figure 1** matrix effect on bastnaesite and zircon is investigated in detail during laser sampling U-Pb
343 dating. The results show that there is significant matrix effect on these minerals. Figure a & b show
344 the weighted average $^{206}\text{Pb}/^{238}\text{U}$ ages of bastnaesite (K-9) and zircon (GJ-1) samples using the zircon
345 standard (91500) as external calibration, while Figure c & d show that of bastnaesite (K-9) and
346 zircon (GJ-1) samples using bastnaesite (K-9) as external calibration standard during the same
347 analytical session, indicating that suitable matrix-matched standard is crucial for *in situ* U-Pb dating
348 of bastnaesite using LA-ICP-MS. The MSWD shows the mean square of weighted deviates.

349

1
2
3
4 350 **Figure 2** Weighted average $^{206}\text{Pb}/^{238}\text{U}$ ages of K-9 bastnaesite calculated during the same analytical
5
6 351 session using 16, 32, 60 μm spot size at repetition rate of 4, 6, 10 Hz and on sample fluence of 4, 6,
7
8 352 10 J/cm^2 under the external standard fixed laser parameter using 44 μm spot size at repetition rate of
9
10
11 353 8 Hz and on sample fluence of 8 J/cm^2 . The MSWD shows the mean square of weighted deviates.
12
13
14 354

15
16 355 **Figure 3** Chondrite-normalized REE distribution pattern of bastnaesite
17
18
19 356

20
21 357 **Figure 4** Tera-Wasserburg plots for *In situ* U-Pb data and ^{207}Pb common lead correction for five
22
23 358 different localities of bastnasites from the Mianning-Dechang belt REE deposits(Sichuan SW China).
24
25
26 359 Error bar is shown 1s errors. These results indicate that the narrow mineralization age of
27
28
29 360 Mianning-Dechang REE belt is consistent with a biotite K-Ar or Ar-Ar age within error.
30
31 361

32
33 362
34
35
36
37
38
39
40
41
42
43
44
45
46
47
48
49
50
51
52
53
54
55
56
57
58
59
60

1
2
3 3634
5 364Table 1. The typical operating conditions for *in situ* U-Pb dating of bastnaesite6
7 365

Agilent 7500a ICP-MS	
RF power	1350 W
Cooling gas	15 L/min
Auxiliary gas	1.0 L/min
Sample gas	0.85 L/min
Ion optic settings	Typical
Detector mode	Dual
Sensitivity	200 Mcps/ppm on ⁸⁹ Y signal via 100 mL/min PFA nebulizer
Integration time	6 ms for Rb, Sr, Ba, Nb, Ta, Zr, Hf and REE, 15 ms for ²⁰⁴ Pb, ²⁰⁶ Pb & ²⁰⁸ Pb, 30 ms for ²⁰⁷ Pb, 10 ms for ²³² Th & ²³⁸ U,
GeoLas 2005 laser ablation system	
Wavelength	193 nm, Excimer laser
Pulse length	15 ns
Energy density	4, 6, 8, 10 J/cm ²
Spot sizes	16, 32, 44, 60 μm
Repetition rate	4, 6, 8, 10 Hz
Carrier gas	Helium (~ 0.85 L/min)

8
9
10
11
12
13
14
15
16
17
18
19
20
21
22
23
24
25
26
27
28
29
30
31
32
33
34
35
36 36637 367
38
39
40
41
42
43
44
45
46
47
48
49
50
51
52
53
54
55
56
57
58
59
60

Table 2 Age comparison with different laser experimental parameters

1. Fluence (changing) (Fixed 44 μm & 8 Hz)	4 J/cm ²	6 J/cm ²	8 J/cm ²	10 J/cm ²
²⁰⁶ Pb/ ²³⁸ U weighted age (Ma)	125.5 \pm 2.0	116.9 \pm 1.6	117.3 \pm 1.5	117.4 \pm 1.5
[MSWD]	[1.07]	[0.73]	[0.50]	[0.33]
[Probability]	[0.38]	[0.68]	[0.88]	[0.97]
2. Spot size (μm) (changing) (Fixed 8 J/cm ² & 8 Hz)	16 μm	32 μm		60 μm
²⁰⁶ Pb/ ²³⁸ U weighted age (Ma)	120.3 \pm 4.8	119.4 \pm 1.4		119.5 \pm 1.2
[MSWD]	[3.6]	[0.34]		[1.18]
[Probability]	[0]	[0.96]		[0.30]
3. Repetition rate (changing) (Fixed 44 μm & 8 J/cm ²)	4 Hz	6 Hz		10 Hz
²⁰⁶ Pb/ ²³⁸ U weighted age (Ma)	116.9 \pm 2.1	117.2 \pm 1.2		118.0 \pm 1.2
[MSWD]	[1.9]	[0.50]		[0.92]
[Probability]	[0.044]	[0.88]		[0.51]

368
369
370371
372
373

374

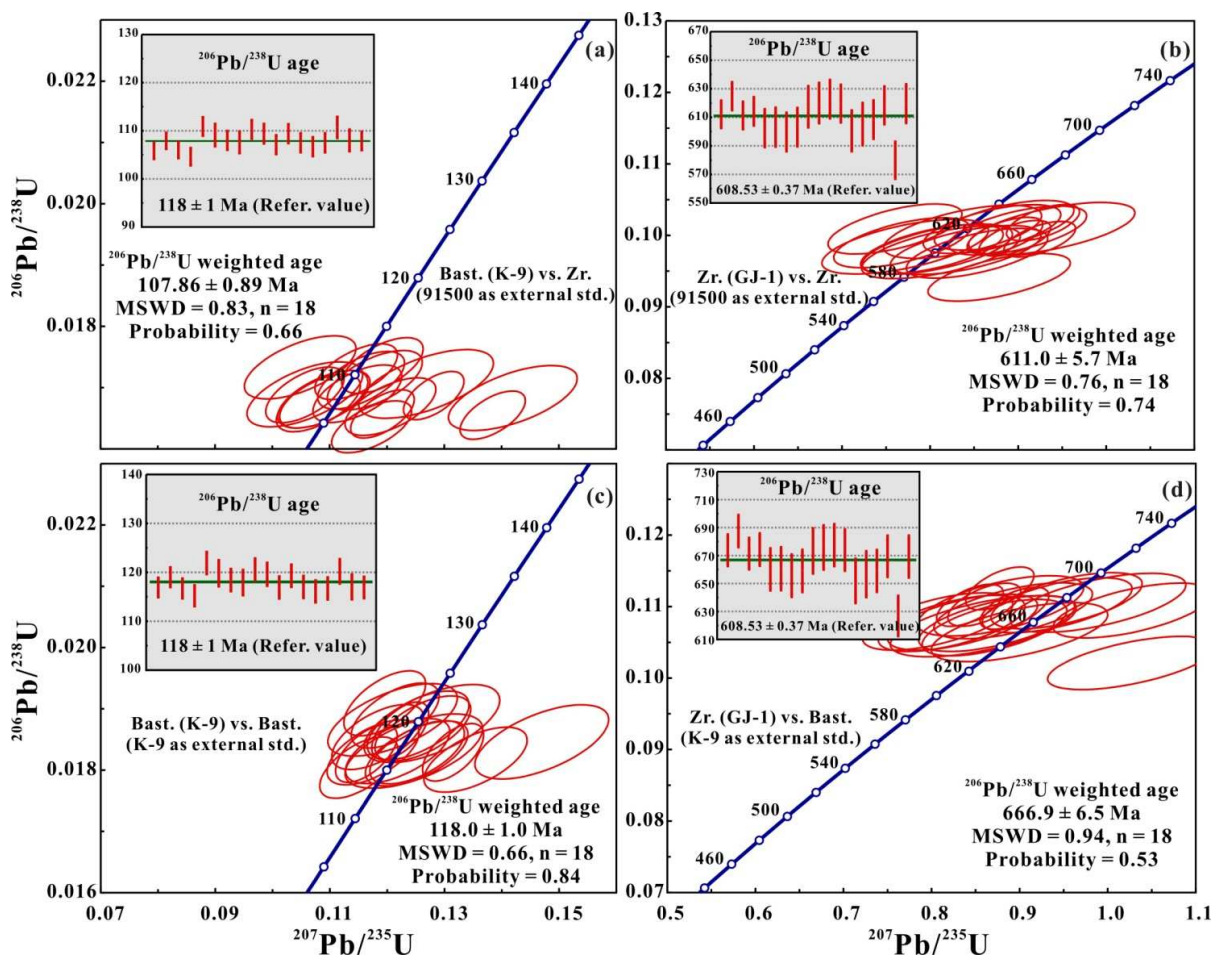


Figure 1

375

376

377

378

379

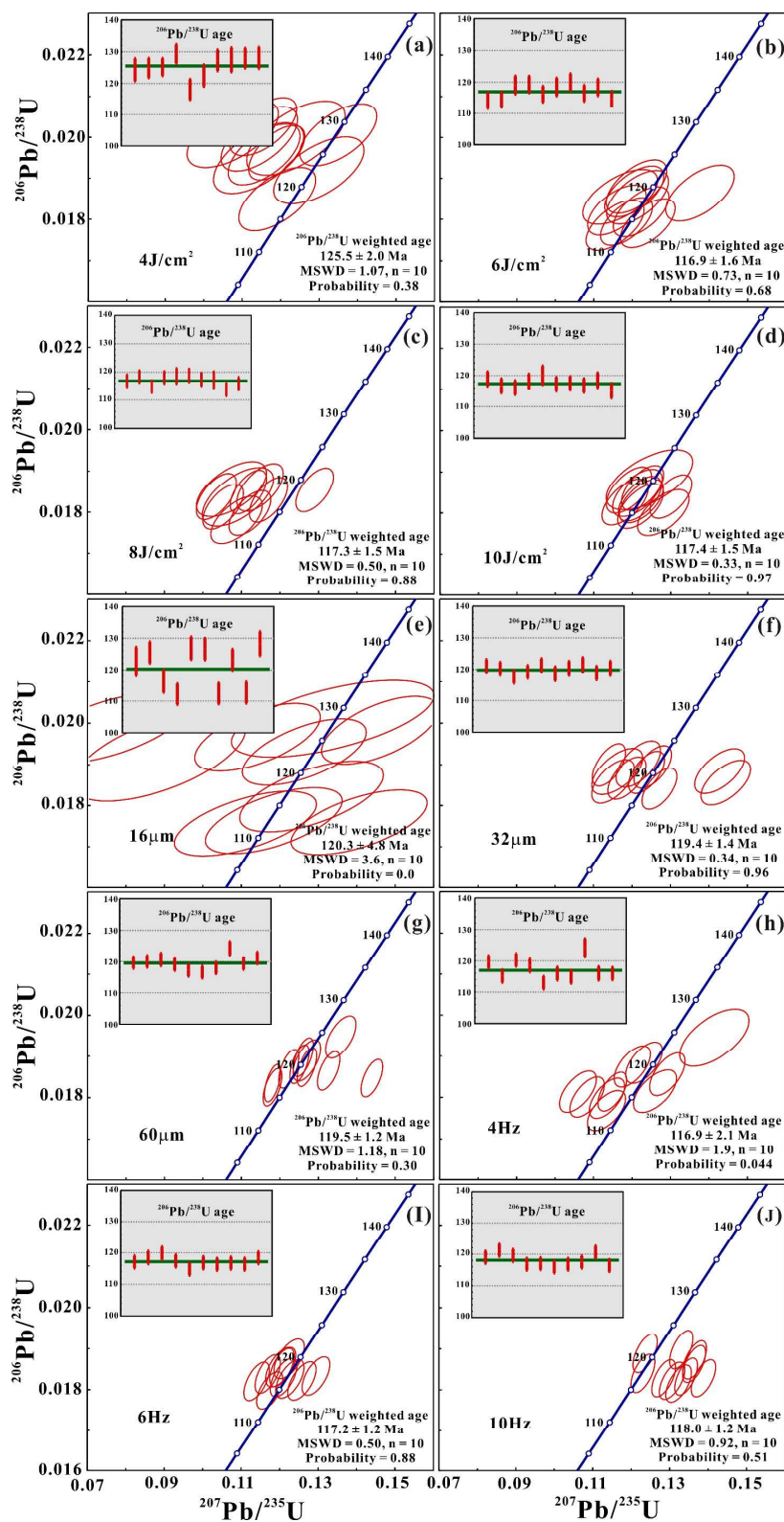


Figure 2

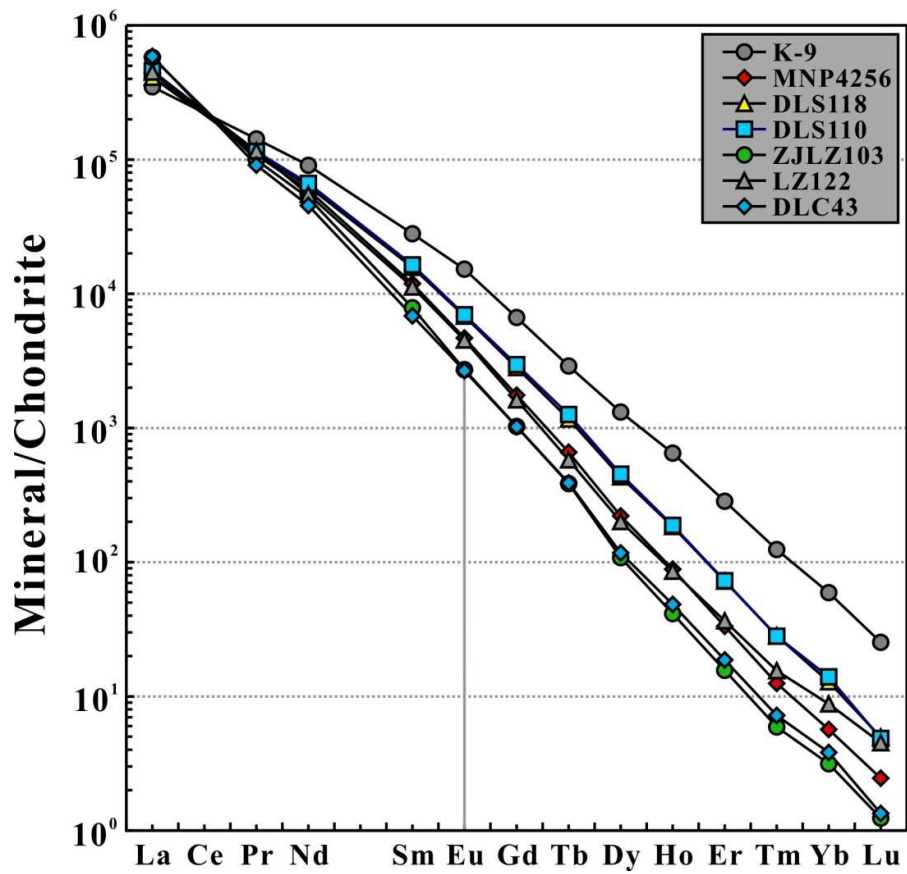
381

382

383

384

385



386

387

388

389

390

Figure 3

391

392

393

394

395

396

397

398

399

400

401

402

403

404

405

406

407

408

409

410

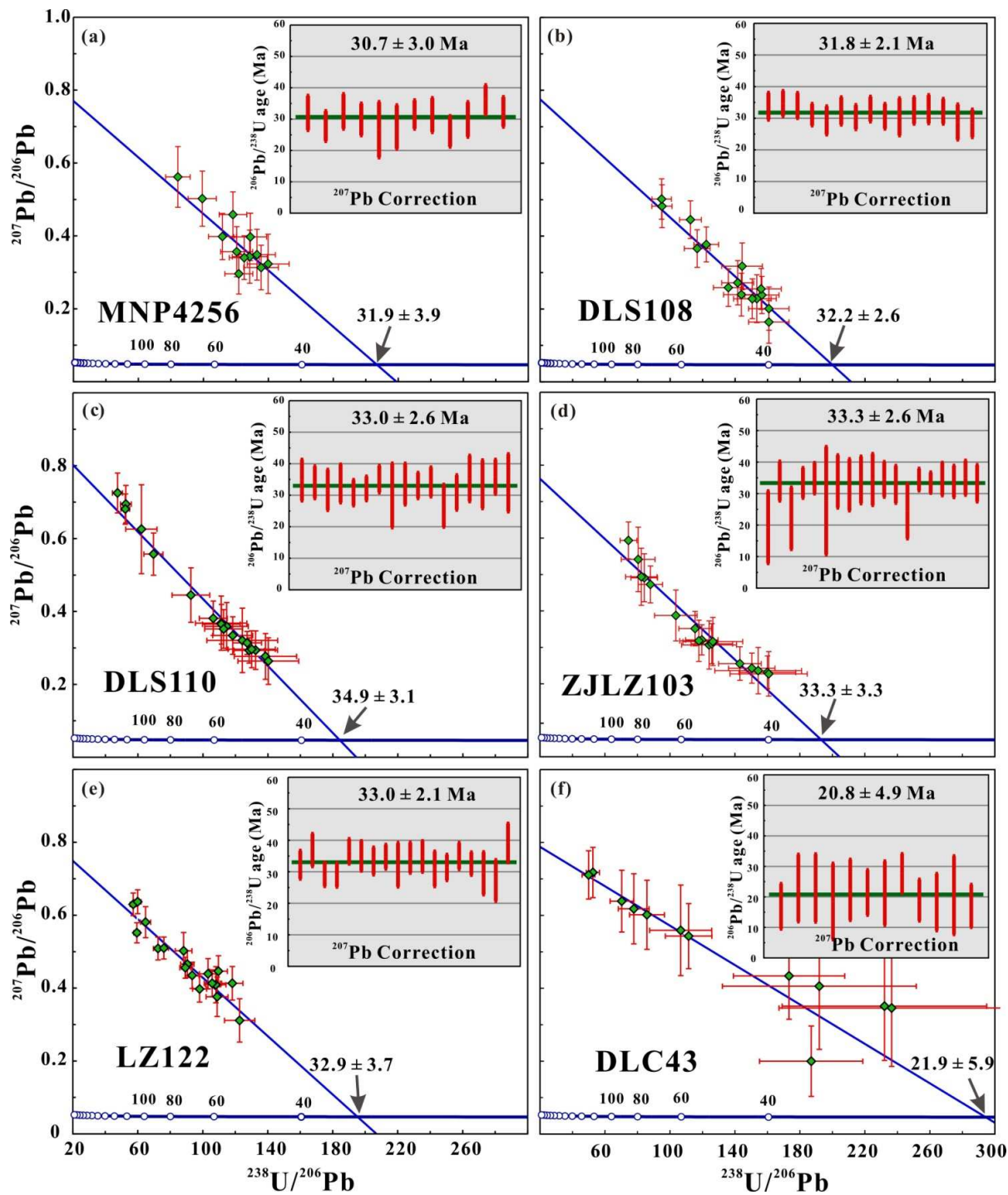


Figure 4

392

393

394

395